

Rh-Doped SrTiO₃ Photocatalyst Electrode Showing Cathodic Photocurrent for Water Splitting under Visible-Light Irradiation

Katsuya Iwashina[†] and Akihiko Kudo^{*,†,‡}

[†]Department of Applied Chemistry, Faculty of Science, Tokyo University of Science, 1-3 Kagurazaka, Shinjuku-ku, Tokyo 162-8601, Japan

[‡]Division of Photocatalyst for Energy and Environment, Research Institute for Science and Technology, Tokyo University of Science, 2641 Noda-shi, Yamazaki, Chiba-ken, Japan 278-8510

S Supporting Information

ABSTRACT: A Rh-doped SrTiO₃ (SrTiO₃:Rh) photocatalyst electrode that was readily prepared by pasting SrTiO₃:Rh powder onto a transparent indium tin oxide electrode gave a cathodic photocurrent under visible-light irradiation ($\lambda > 420$ nm), indicating that the SrTiO₃:Rh photocatalyst electrode possessed p-type semiconductor character. The cathodic photocurrent increased with an increase in the amount of doped Rh up to 7 atom %. The incident-photon-to-current efficiency at 420 nm was 0.18% under an applied potential of -0.7 V vs Ag/AgCl for the SrTiO₃:Rh(7 atom %) photocatalyst electrode. The photocurrent was confirmed to be due to water splitting by analyzing the evolved H₂ and O₂. The water splitting proceeded with the application of an external bias smaller than 1.23 V versus a Pt counter electrode under visible-light irradiation and also using a solar simulator, suggesting that solar energy conversion should be possible with the present photoelectrochemical water splitting.

Solar water splitting for clean hydrogen production using photoelectrodes and powdered photocatalysts has been paid attention from the viewpoint of an energy issue. Several new materials to serve as powdered photocatalysts for water splitting have recently been developed,^{1,2} whereas materials for photoelectrodes are still limited. The representative TiO₂ photoelectrode possesses a band gap of 3.0 eV and an insufficient conduction band level for H₂ production. Therefore, it requires UV light and an external bias for water splitting.³ SrTiO₃ and KTaO₃ are semiconductor photoelectrodes that can split water with no external bias under UV irradiation because their conduction band levels are higher than the redox potential for H₂ evolution.⁴ WO₃,^{5,6} Fe₂O₃,⁷ and BiVO₄^{8–11} semiconductor photoelectrodes have been extensively studied because of their visible-light responses. TaON,¹² Ta₃N₅,¹³ and LaTiO₂N¹⁴ of (oxy)nitride photoelectrodes have also been reported for water splitting under visible-light irradiation. These semiconductor photoelectrodes possess n-type character. Stable oxide semiconductor electrodes with p-type character for water splitting have not been reported, except for CaFe₂O₄.¹⁵ The development of stable oxide semiconductor materials with p-type character is important not only for water-splitting electrodes but also for electronics, optoelectronics, and solar cells.

Powdered SrTiO₃ photocatalyst is active for water splitting under UV irradiation.^{16,17} We have developed transition-metal-doped SrTiO₃ photocatalysts for H₂ and O₂ evolution in the presence of reducing and oxidizing reagents, respectively, under visible-light irradiation.^{1,18} Among them, Rh-doped SrTiO₃ (SrTiO₃:Rh) is a highly active oxide photocatalyst for sacrificial H₂ evolution under visible-light irradiation.¹⁹ Moreover, it works as an H₂-evolving photocatalyst in Z-scheme systems combined with O₂-evolving photocatalysts such as BiVO₄, WO₃, and Bi₂MoO₆ for solar water splitting in the presence and absence of electron mediators.²⁰ Thus, SrTiO₃:Rh is an attractive material for solar energy conversion and is expected to function as a photoelectrode material for water splitting under visible-light irradiation.

In the present study, we examined photoelectrochemical properties of powdered SrTiO₃:Rh photocatalyst loaded on an indium tin oxide (ITO) electrode to demonstrate water splitting under visible-light irradiation.

SrTiO₃ powder doped with x mol % Rh ($0 \leq x \leq 10$) at Ti sites was prepared by a solid-state reaction. The starting materials, SrCO₃ (Kanto Chemical; 99.9%), TiO₂ (Soekawa Chemical; 99.9%), and Rh₂O₃ (Wako Pure Chemical), were mixed in a Sr:Ti:Rh ratio of 1.07:(1 - x): x . The mixture was calcined in air at 1173 K for 1 h and then at 1373 K for 10 h in an aluminum crucible. The crystalline form of the obtained powder was confirmed by X-ray diffraction (Rigaku; MiniFlex). SrTiO₃:Rh photocatalyst electrodes were prepared by a squeegee method that coated a paste composed of 20 mg of SrTiO₃:Rh photocatalyst powder, 20 μ L of acetylacetone (Kanto Chemical; 99.5%), and 40 μ L of distilled water onto a transparent ITO electrode and then calcined at 573 K for 2 h in air. The apparent area on the electrode coated with the SrTiO₃:Rh photocatalyst powder was 1–3 cm². Scanning electron microscopy (SEM) images of the electrode are shown in Figure S1 in the Supporting Information. An ITO electrode was partially covered with SrTiO₃:Rh powder. The deposited SrTiO₃:Rh did not form a sintered thin film. Thus, the photoelectrochemical property obtained was that of powdered samples, reflecting the properties of powdered photocatalysts, so we call it photocatalyst electrode. Diffuse reflection spectra were obtained using a UV–vis–NIR spectrometer (JASCO; UbestV-570) and were converted from reflection to absorbance by the Kubelka–Munk method. Photoelectrochemical properties were evaluated using a potentiostat

Received: June 1, 2011

Published: July 28, 2011

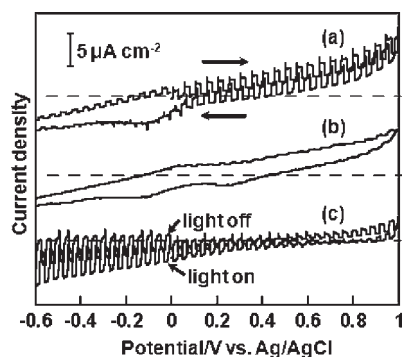


Figure 1. Current vs potential curves for (a) SrTiO₃ ($\lambda > 300$ nm), (b) SrTiO₃ ($\lambda > 420$ nm), and (c) SrTiO₃:Rh(1 atom %) ($\lambda > 420$ nm) electrodes. Electrolyte, 0.1 mol L⁻¹ aqueous K₂SO₄ solution; sweep rate, 20 mV s⁻¹; light source, 300 W Xe lamp.

(Hokuto Denko; HZ-3000 or HZ-5000) and an H-type cell divided into working and counter electrode compartments by Nafion 117 (Dupont). Platinum, a saturated Ag/AgCl electrode (DKK-TOA), and 0.1 mol L⁻¹ aqueous solution of K₂SO₄ (Kanto Chemical; 99.0%) were used as the counter electrode, reference electrode, and electrolyte, respectively. The electrolyte in both compartments was bubbled with N₂ or Ar before measurements. The light source was a Xe lamp (PerkinElmer; Cermax-PE300BF). The wavelength of the incident light was controlled by cutoff filters (HOYA), an NIR-absorbing filter (Sigma Koki; CCF-50S-500C), and a plano-convex lens (Sigma Koki; SLSQ-60-150P). A solar simulator with an air-mass 1.5 filter (Pecell Technologies; PEC-L11, 100 mW cm⁻²) was also used for photoelectrochemical measurements. The amounts of evolved H₂ and O₂ were determined using an online gas chromatograph (Shimadzu; GC-8A, MS-5A column, thermal conductivity detector, Ar carrier) and an Ar-flow reaction cell (10 mL min⁻¹).

Figure 1 shows the photoresponse in the current–potential curves for SrTiO₃ and SrTiO₃:Rh(1 atom %) electrodes. SrTiO₃ gave an anodic photocurrent under only UV irradiation, indicating n-type character as reported previously.⁴ This result indicated that the easy preparation method of the electrode employed in the present study was available. In contrast, the SrTiO₃:Rh(1 atom %) electrode showed a cathodic photocurrent with an onset potential at 0.6 V vs Ag/AgCl. This result suggested that the SrTiO₃:Rh(1 atom %) electrode possessed p-type character. The ITO surface was considerably exposed to the electrolyte, as suggested by SEM (Figure S1). Therefore, the photoresponse of a bare ITO electrode was measured as a control experiment. The anodic photocurrent of ITO under UV irradiation was negligible in comparison with that of nondoped SrTiO₃. Moreover, a cathodic photocurrent was not observed at all for the ITO electrode under UV and visible-light irradiation. Therefore, the photoresponse observed in Figure 1 was not due to the ITO electrode.

The stable oxidation states of a Rh dopant in oxides are trivalent and tetravalent.¹⁹ These Rh species reversibly change depending on the conditions:



Rh³⁺ and Rh⁴⁺ are doped at Ti⁴⁺ sites. When trivalent Rh is doped without accompanying formation of oxygen vacancies,

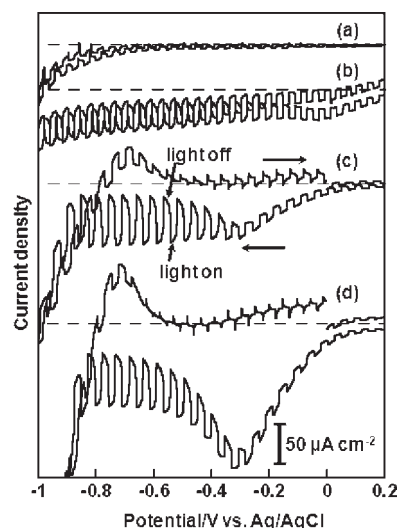


Figure 2. Current vs potential curves of SrTiO₃:Rh(*x* atom %) for *x* = (a) 1, (b) 4, (c) 7, and (d) 10. Electrolyte, 0.1 mol L⁻¹ aqueous K₂SO₄ solution; sweep rate, 20 mV s⁻¹; light source, 300 W Xe lamp with an L42 cutoff filter.

it gives a hole due to charge compensation (eq 1), analogous to Li⁺-doped Ni^{II}O that is a typical p-type metal oxide semiconductor. On the other hand, if tetravalent Rh is doped, it easily releases a hole because of the easy reversibility of changes in the oxidation number of Rh in oxides (eq 2). It is considered that the p-type character appeared according to these schemes.

Figure 2 shows visible-light responses in the current–potential curves for SrTiO₃ electrodes doped with different amounts of Rh. X-ray diffraction measurements revealed that SrTiO₃:Rh was obtained as a single phase, although SrTiO₃:Rh(7 atom %) and SrTiO₃:Rh(10 atom %) contained very small amounts of impurities (Figure S2). Reduction waves observed around -0.3 V vs Ag/AgCl under dark conditions would be due to the reduction of Rh⁴⁺ in SrTiO₃:Rh and/or the impurities. The cathodic photocurrent increased with an increase in the amount of doped Rh. This is due to the increase in the absorption coefficient near 400 nm that contributes to the visible-light response (Figure S3). The optimum amount of doped Rh was 7 atom % for the present photoelectrode, whereas it was 1 atom % for a powdered photocatalyst. Doped Rh contributes not only as a visible-light absorber but also as a recombination center for photogenerated electrons and holes. The efficiencies of the photoelectrodes and the photocatalysts are determined by the balance of these factors of light absorption and recombination. In the photoelectrochemical system, applying an external bias and forming a band bending assist the charge separation and suppress the recombination, while such assistance is not expected for the powdered system. As a result, the optimum amount of Rh dopant for the electrochemical system was larger than that for the powdered system.

Figure 3 shows diffuse reflectance spectra of SrTiO₃ and SrTiO₃:Rh(7 atom %) powder and the wavelength dependence of the cathodic photocurrent over the SrTiO₃:Rh(7 atom %) electrode using cutoff filters. In principle, the energy diagram of the present electrode should be the same as that of the powdered photocatalyst (except for band bending) because the photocatalyst electrode is employed as shown by the SEM image in Figure S1. Therefore, the detailed energy diagram for the SrTiO₃:Rh photocatalyst shown in ref 19 can be applied to the present

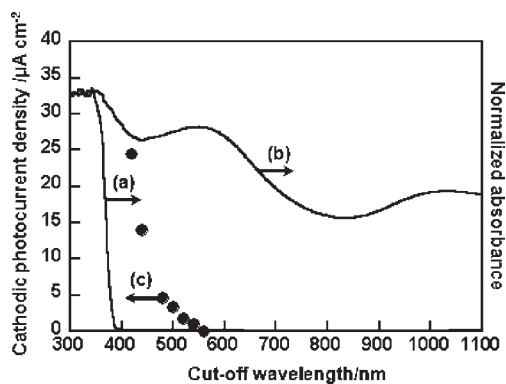


Figure 3. Diffuse reflectance spectra of (a) SrTiO₃ and (b) SrTiO₃:Rh(7 atom %) powders and (c) dependence of the cathodic photocurrent density over the SrTiO₃:Rh(7 atom %) electrode upon the cutoff wavelength of the incident light. Electrolyte, 0.1 mol L⁻¹ aqueous K₂SO₄ solution; applied potential, -0.8 V vs Ag/AgCl; light source, 300 W Xe lamp with cutoff filters.

electrode system. SrTiO₃:Rh(7 atom %) possessed visible-light absorption bands that were not observed for nondoped SrTiO₃. The visible-light absorption band at ~400 nm is due to electronic transitions from electron-donor levels consisting of Rh³⁺ to a conduction band of SrTiO₃, while that at ~600 nm is assigned to transitions from a valence band of SrTiO₃ to acceptor levels consisting of Rh⁴⁺.¹⁹ The absorption band at ~1000 nm is assigned to d-d or charge transfer transitions between trivalent and tetravalent Rh species. The cathodic photocurrent was observed at wavelengths ≤540 nm. This photoresponse is due to electronic transitions from electron donor levels consisting of Rh³⁺ to a conduction band of SrTiO₃, in agreement with that of photocatalytic reactions for sacrificial H₂ evolution¹⁹ and water splitting using a Z-scheme system.²⁰ Other absorption bands in the visible and NIR regions of SrTiO₃:Rh and impurities did not give any photoresponse.

It is indispensable to check the evolution of H₂ and O₂ for photoelectrochemical water splitting^{12,15} because it is not always guaranteed that the observed photocurrent is due to water splitting. Therefore, water splitting was carried out using a SrTiO₃:Rh(7 atom %) photocatalyst electrode to check whether the observed cathodic photocurrent seen in Figure 2 was due to water reduction to form H₂ or reduction of the electrode itself. The cathodic photocurrent was observed at -0.5 V vs Ag/AgCl for longer than 16 h under visible-light irradiation, as shown in Figure 4. Faradaic efficiencies for H₂ and O₂ evolution were 100% within experimental error, indicating that the observed photocurrent was due to water splitting. Although a significant decrease in the photocurrent was observed at the beginning stage, it became stable after several hours. No significant difference in the SEM images before and after the photoelectrolysis was observed (Figure S1). This result excluded the possibility that peeling of the powdered SrTiO₃:Rh from the ITO was the reason for the degradation. The degradation of the photocurrent is thought to be due to the change in the surface state. The incident-photon-to-current efficiency of the SrTiO₃:Rh(7 atom %) photocatalyst electrode was 0.18% at 420 nm under an applied potential of -0.7 V vs Ag/AgCl. An external bias has to be smaller than 1.23 V vs the counter electrode (the theoretical voltage for electrolysis of water) if conversion of light energy is taken into account. The water splitting proceeded even when an

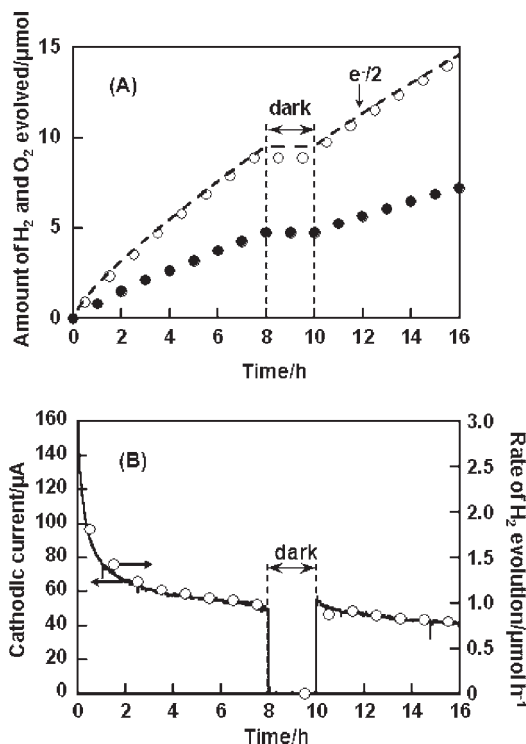


Figure 4. (A) H₂ (○) and O₂ (●) evolution and half of the number of electrons passed through an outer circuit (dashed line) by photoelectrochemical water splitting using a SrTiO₃:Rh(7 atom %) electrode under visible-light irradiation with an applied potential of -0.5 V vs Ag/AgCl. (B) Stability of the cathodic photocurrent (solid curve) and the rate of H₂ evolution (○) for the water splitting. Apparent electrode area, 1.2 cm²; electrolyte, 0.1 mol L⁻¹ aqueous K₂SO₄ solution; light source, 300 W Xe lamp with an L42 cutoff filter.

external bias of -0.5 V vs the Pt counter electrode was applied, as shown in Figure S4. Moreover, the cathodic photocurrent was observed for a time longer than 30 h at -0.8 V vs the Pt counter electrode using a solar simulator, as shown in Figure S5. These results indicate that the SrTiO₃:Rh photocatalyst electrode is functional for solar energy conversion through water splitting. The efficiency is expected to be improved by examination of the preparation method of the electrode and loading of cocatalysts.

In conclusion, Rh-doped SrTiO₃ (SrTiO₃:Rh) photocatalyst electrodes gave a visible-light response and exhibited p-type semiconductor character, producing a cathodic photocurrent under visible-light irradiation up to 540 nm. Water splitting under visible-light irradiation was achieved by making an electrode using a powdered SrTiO₃:Rh photocatalyst, although the water splitting did not proceed in the suspended form using the powder. SrTiO₃:Rh has arisen as a promising semiconductor photoelectrode for solar water splitting.

■ ASSOCIATED CONTENT

S Supporting Information. SEM images of the SrTiO₃:Rh(7 atom %) electrode surface, X-ray diffraction patterns and diffuse reflectance spectra of SrTiO₃:Rh powders, and photoelectrochemical water splitting results using a 300 W Xe lamp with an L42 cutoff filter or a solar simulator. This material is available free of charge via the Internet at <http://pubs.acs.org>.

■ AUTHOR INFORMATION

Corresponding Author

a-kudo@rs.kagu.tus.ac.jp

■ ACKNOWLEDGMENT

This work was supported by ENEOS Hydrogen Foundation and a Grant-in-Aid for Priority Area Research from the Ministry of Education, Culture, Sports, Science, and Technology of Japan. The authors dedicate this article to the memory of Professor Ken-ichi Honda, a pioneer in this research area, who passed away in 2011.

■ REFERENCES

- (1) Kudo, A.; Miseki, Y. *Chem. Soc. Rev.* **2009**, *38*, 253–278.
- (2) Osterloh, E. F. *Chem. Mater.* **2008**, *20*, 35–54.
- (3) Fujishima, A.; Honda, K. *Nature* **1972**, *238*, 37–38.
- (4) (a) Wrighton, S. M.; Ellis, B. A.; Wolczanski, T. P.; Morse, L. D.; Abrahamson, B. H.; Ginley, S. D. *J. Am. Chem. Soc.* **1976**, *98*, 2774–2779. (b) Ellis, B. A.; Kaiser, W. S.; Wrighton, S. M. *J. Phys. Chem.* **1976**, *80*, 1325–1328.
- (5) (a) Spichiger-Ulmann, M.; Augustynski, J. *J. Appl. Phys.* **1983**, *54*, 6061–6064. (b) Santato, C.; Ulmann, M.; Augustynski, J. *J. Phys. Chem. B* **2001**, *105*, 936–940.
- (6) Miller, L. E.; Marden, B.; Cole, B.; Lum, M. *Electrochem. Solid-State Lett.* **2006**, *9*, G248–G250.
- (7) (a) Duret, A.; Grätzel, M. *J. Phys. Chem. B* **2005**, *109*, 17184–17191. (b) Sivula, K.; Formal, L. F.; Grätzel, M. *ChemSusChem* **2011**, *4*, 432–449.
- (8) (a) Sayama, K.; Nomura, A.; Zou, Z.; Abe, R.; Abe, Y.; Arakawa, H. *Chem. Commun.* **2003**, 2908–2909. (b) Sayama, K.; Nomura, A.; Arai, T.; Sugita, T.; Abe, R.; Yanagida, M.; Oi, T.; Iwasaki, Y.; Abe, Y.; Sugihara, H. *J. Phys. Chem. B* **2006**, *110*, 11352–11360. (c) Sayama, K.; Wang, N.; Miseki, Y.; Kusama, H.; Onozawa-Komatsuzaki, N.; Sugihara, H. *Chem. Lett.* **2010**, *39*, 17–19.
- (9) Long, M.; Cai, W.; Kisch, H. *J. Phys. Chem. C* **2008**, *112*, 548–554.
- (10) Iwase, A.; Kudo, A. *J. Mater. Chem.* **2010**, *20*, 7536–7542.
- (11) Berglund, P. S.; Flaherty, W. D.; Hahn, T. N.; Bard, J. A.; Mullins, B. C. *J. Phys. Chem. C* **2011**, *115*, 3794–3802.
- (12) (a) Abe, R.; Takata, T.; Sugihara, H.; Domen, K. *Chem. Lett.* **2005**, *34*, 1162–1163. (b) Abe, R.; Higashi, M.; Domen, K. *J. Am. Chem. Soc.* **2010**, *132*, 11828–11829.
- (13) Ishikawa, A.; Takata, T.; Kondo, N. J.; Hara, M.; Domen, K. *J. Phys. Chem. B* **2004**, *108*, 11049–11053.
- (14) Nishimura, N.; Raphael, B.; Maeda, K.; Gendre, L. L.; Abe, R.; Kubota, J.; Domen, K. *Thin Solid Films* **2010**, *518*, 5855–5859.
- (15) (a) Matsumoto, Y.; Omae, M.; Sugiyama, K.; Sato, E. *J. Phys. Chem.* **1987**, *91*, 577–581. (b) Ida, S.; Yamada, K.; Hagiwara, H.; Matsumoto, Y.; Ishihara, T. *J. Am. Chem. Soc.* **2010**, *132*, 17343–17345.
- (16) (a) Domen, K.; Naito, S.; Soma, M.; Onishi, T.; Tamaru, K. *J. Chem. Soc., Chem. Commun.* **1980**, 543–544. (b) Domen, K.; Kudo, A.; Onishi, T.; Kosugi, N.; Kuroda, H. *J. Phys. Chem.* **1986**, *90*, 292–295.
- (17) Lehn, J. M.; Sauvage, J. P.; Zissel, R.; Hilaire, L. *Isr. J. Chem.* **1982**, *22*, 168.
- (18) Kudo, A.; Niishiro, R.; Iwase, A.; Kato, H. *Chem. Phys.* **2007**, *339*, 104–110.
- (19) Konta, R.; Ishii, T.; Kato, H.; Kudo, A. *J. Phys. Chem. B* **2004**, *108*, 8992–8995.
- (20) (a) Kato, H.; Hori, M.; Konta, R.; Shimodaira, Y.; Kudo, A. *Chem. Lett.* **2004**, *33*, 1348–1349. (b) Sasaki, Y.; Iwase, A.; Kato, H.; Kudo, A. *J. Catal.* **2008**, *259*, 133–137. (c) Sasaki, Y.; Nemoto, H.; Saito, K.; Kudo, A. *J. Phys. Chem. C* **2009**, *113*, 17536–17542. (d) Kudo, A. *MRS Bull.* **2011**, *36*, 32–38.